

Amphibolite *vs.* banded amphibolite: a case study in the São Martinho-Arronches area, Tomar Cordoba Shear Zone, NE Ossa Morena Zone, Portugal

Anfibolita *versus* anfibolita bandeada: el caso de São Martinho-zona de Arronches, Zona de Cizalla de Tomar Cordoba, Zona NE de Ossa Morena, Portugal

DE OLIVEIRA, D. P. S.¹; WIECHOWSKI, A.²; ROBB, L. J.³ & INVERNO, C. M. C.⁴

Abstract

Amphibolites and banded amphibolites form an integral part of the Série Negra rocks that outcrop within the Tomar Cordoba Shear Zone that forms the boundary between the Ossa Morena Zone and the Central Iberian Zone. The terms *amphibolite* and "*amphibole schist*" (here changed to *banded amphibolite*) have been regularly used by exploration geologists when referring to the amphibolitic-type lithologies, with or without a marked schistosity, that outcrop in the Ossa Morena Zone, e.g. in the vicinity of the São Martinho gold prospect. In this study the term *amphibolite* is used for homogeneous, massive-texture rocks at the mesoscopic scale whereas *banded amphibolite* refers to rocks that exhibit a distinct banding at the outcrop scale. Microscopically both rock types show a schistosity, which is better defined in the banded amphibolites. These rock types have a rather similar mineralogy. Geochemically, in terms of their major element composition, there is little difference between them. However, each exhibits a distinct mineral chemistry: the amphiboles in the amphibolites are actinolite-magnesiohornblende while those in the banded amphibolites are mostly magnesiohornblende and minor tschermakite. Likewise, the feldspars in the amphibolites plot in the oligoclase-andesine and labradorite-bytownite fields while those in the banded amphibolites are largely constrained to the labradorite fields with a few outliers in the andesine and bytownite fields.

Tentative geochemical signatures for protolith nature and tectonic setting indicate a probable basic protolith for both amphibolites and banded amphibolites although the textures preserved in the banded amphibolites may also indicate a sedimentary-tuffaceous origin.

Key words: Amphibolite, banded amphibolite, Série Negra, Tomar Cordoba Shear Zone, NE Ossa Morena Zone.

- (1) Economic Geology Research Institute-Hugh Allsopp Laboratory (EGRI-HAL), University of the Witwatersrand, Private Bag 3, WITS 2050, Rep. South Africa. Present address: Instituto Geológico e Mineiro, Apartado 7586, 2721-866 Alfragide (Lisbon), Portugal
- (2) Department of Mineralogy and Ore Deposit Research, RWTH Aachen, Wüllnerstr. 2, D-52062 Aachen, Germany
- (3) Economic Geology Research Institute-Hugh Allsopp Laboratory (EGRI-HAL). University of the Witwatersrand, Private Bag 3, WITS 2050, Rep. South Africa
- (4) Instituto Geológico e Mineiro, Apartado 7586, 2721-866 Alfragide (Lisbon), Portugal

1. Introduction

The terms *amphibolite versus "amphibole schist"* (here modified to banded amphibolite) have been regularly used by gold exploration companies operating in the Iberian Ossa Morena Zone (e.g. Rio Tinto Zinc, Portuglobal-Explorações Mineiras, Lda., Auspex Minerals Ltd.) when referring to the amphibolitic-type lithologies that outcrop in the gold prospect areas, as is the case of São Martinho, east of Alter do Chão. These amphibolitic-type lithologies (*s.l.*) are locally hosts to (significant) gold mineralisation on their own or at the transition between them and quartz biotite schists of the Série Negra (de OLIVEIRA, 2001).

In São Martinho, amphibolites and banded amphibolites at times outcropping adjacent to each other, form part of the Série Negra rocks that outcrop within the Tomar Cordoba Shear Zone (TCSZ) in the NE Ossa Morena Zone. The amphibolites and banded amphibolites outcrop south of the Blastomylonitic Belt where the Série Negra rocks have reached amphibolite facies metamorphism as opposed to those outcropping north of the Blastomylonitic Belt that have only reached greenschist facies metamorphic grade. In light of the potential economic importance of these rocks and the distinction between the terms amphibolite and banded amphibolite ("*amphibole schist*") that have crept into company reports on the area and other metallogenic studies, this paper, that does not intend to be a paper on fine metamorphic petrology, examines and records differences in texture, bulk geochemistry and mineral chemistry

between amphibolites and banded amphibolites and makes tentative observations regarding the protolith nature of these rocks from samples collected from outcrop and trenches in the area (figure 1) to investigate whether the differences observed at the mesoscopic scale are also evident at the microscopic scale, in view of the economic gold potential of these rocks in the area.

2. GEOLOGICAL AND STRUCTURAL SETTING

The study area is located within a polygon that has at its extreme limits the towns of Alter do Chão and Arronches in the W and SE respectively (figures 1 and 2). The Série Negra (*Black Series*) is a package consisting of metasedimentary (metaarenites and metapelites), basic igneous (amphibolites and banded amphibolites) and felsic volcanic (metarhyolites) rocks (e.g. OLIVEIRA *et al.*, 1991; de OLIVEIRA, 2001). The Série Negra occurs juxtaposed on both the north and south limbs of an asymmetric flower structure that contains, from north to south, low-grade metamorphic rocks (greenschist facies) to intermediate-grade metamorphic rocks (amphibolite facies) separated by a central corridor of high-grade metamorphic rocks (the Blastomylonitic Belt; figure 2) christened initially as the TCSZ. The TCSZ is, however, conventionally understood today to be the zone located immediately southwards of the Central Iberian Zone up to and including the Barreiros tectonised granitoids (e.g. OLIVEIRA *et al.*, 1991; figure 2).

The TCSZ is a geologically complex and diverse zone of intense deformation

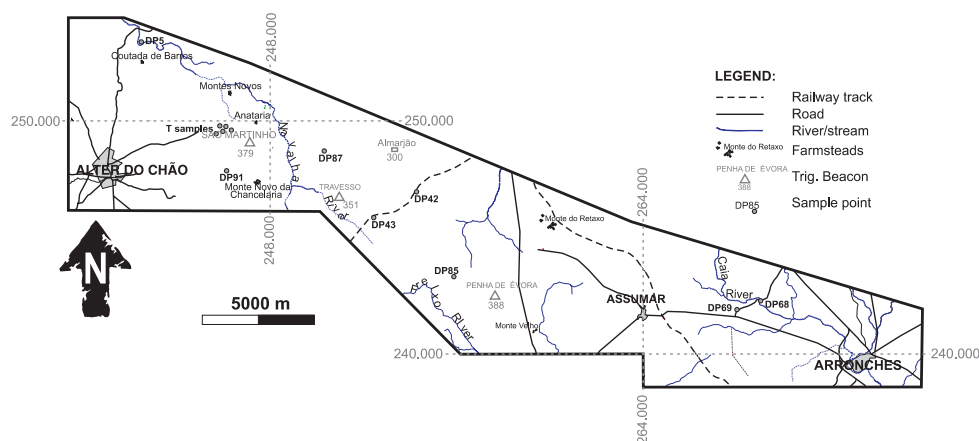


Figure 1. Polygon of the São Martinho-Arronches area with sample locations.

and metamorphism contemporaneous with a large sinistral displacement, which may be due to a large intracontinental sinistral fault active during the Variscan Orogeny (BERTHÉ *et al.*, 1979) with sinistral displacements of 100 (BURG *et al.*, 1981) to 300 km (ABALOS & EGUÍLUZ, 1992). This displacement caused mylonitisation and retrograde metamorphism (under greenschist to amphibolite facies) to all previous structures and mineral assemblages (QUESADA & MUNHÁ, 1990). PEREIRA & SILVA (2001) considered the Tomar Cordoba Shear Zone a major Eohercynian-Hercynian sinistral transcurrent fault overprinting a Cadomian arc localised at a convergent margin of Gondwana.

The Portuguese sector of the TCSZ comprises a series of polymetamorphic structural-tectonic subdomains defined by PEREIRA in 1995 and 1999. These subdomains are, from north to south, Urra-Mosteiros-Ouguela Subdomain, Degolados-Campo Maior Subdomain, Arronches-

Morenos-Caia Subdomain, Assumar Subdomain and the Alter do Chão-Elvas Subdomain. Each of these subdomains is a thrust fault-bounded package of rocks and the thrust faults and vergence are arranged in a flower structure more or less centered in the Blastomylonitic Belt (figure 1).

The Blastomylonitic Belt (approximately the core of this flower structure) is made up primarily of Palaeoproterozoic age [2237 and 1700 Ma, by de OLIVEIRA *et al.*, (2002) and ORDOÑES-CASADO (1998), respectively] migmatitic gneisses of the Campo Maior Formation.

Within the TCSZ outcrops the Neoproterozoic Série Negra rocks (maximum age for the final stages of sedimentation, ca. 565 Ma; SCHÄFFER *et al.*, 1993); the name derived as a result of the overwhelming majority of dark-coloured rocks that make up this series. The Série Negra outcrops scarcely both north and south of the Blastomylonitic Belt. Stratigraphically the Série Negra is made

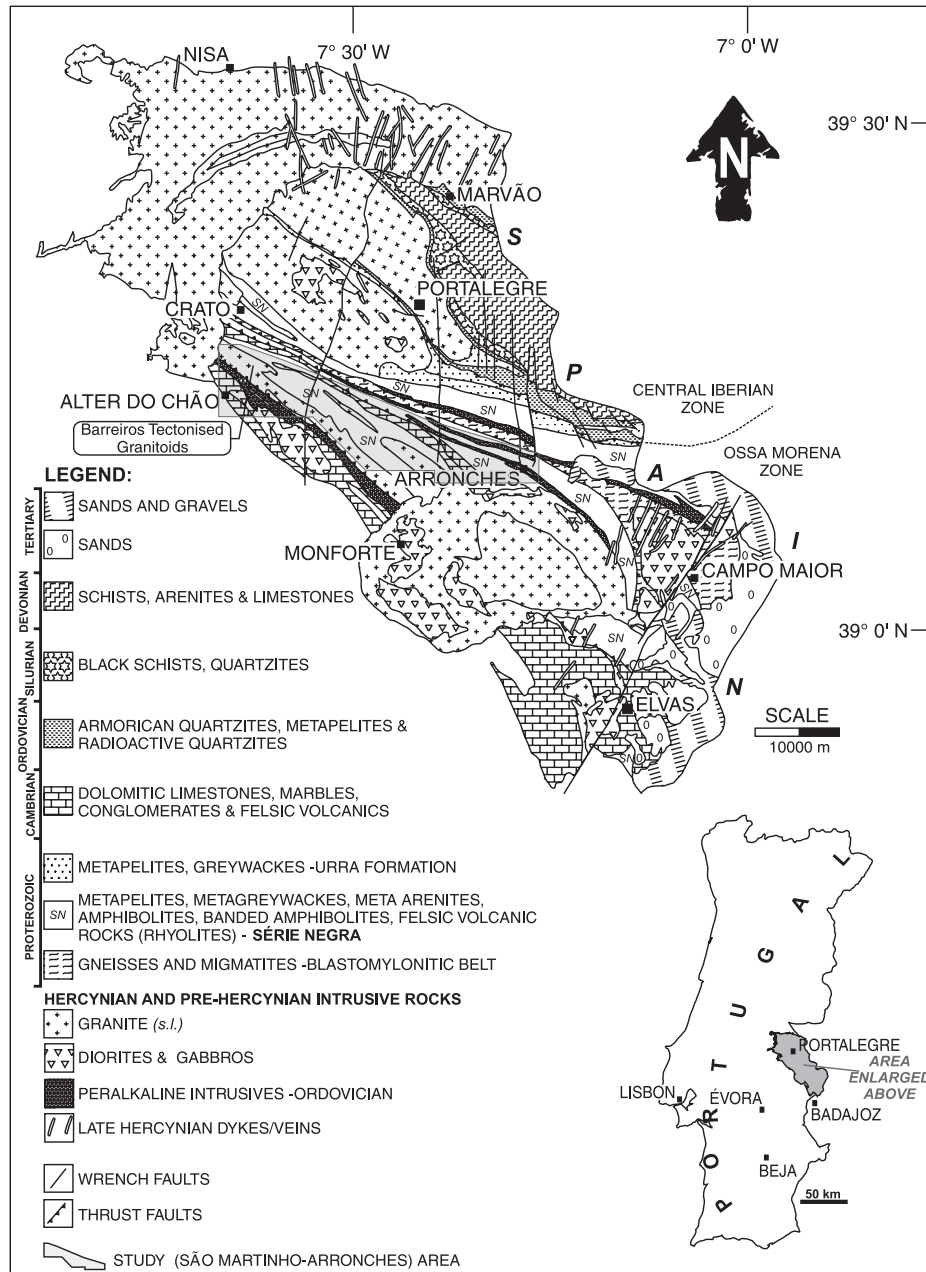


Figure 2. Excerpt from the 1:500000 geological map of Portugal showing the simplified geology of the NE Ossa Morena and SE Central Iberian Zones (adapted after OLIVEIRA *et al.*, 1992). The shaded area corresponds to the location of the study area that is located south of the Blastomylonitic Belt in amphibolite facies-grade metamorphic rocks (adapted after de OLIVEIRA, 2001).

up of the (lower) Morenos and (upper) Mosteiros Formations (OLIVEIRA, *et al.*, 1991). The Morenos Formation is made up of micaceous schists that are locally garnet-bearing, limestones and calc-silicate assemblages, meta-arkoses, meta-arenites (quartzites) and micaceous and siliceous schists, amphibolites and pyroclastic rocks (OLIVEIRA *et al.*, 1991). The Mosteiros Formation consists of black schists/slates, greywackes, black cherts (quartzites?), limestones and amphibolites (OLIVEIRA *et al.*, 1991). North of the Blastomylonitic Belt and unconformably overlying the Mosteiros Formation occurs the Urroa Formation made up of a lower porphyry unit and an upper pelite/greywacke unit (OLIVEIRA *et al.*, 1991) usually of a pale green colour (de Oliveira, 1998). At the TCSZ borders, a (Lower) Cambrian sequence of platform sediments is preserved, which unconformably overlies the Neoproterozoic Série Negra meta-sedimentary rocks (see figure 1) and consists of micaceous schists, amphibolites, metamorphosed carbonate rocks and pelitic schists (OLIVEIRA *et al.*, 1991; PEREIRA, 1995).

The amphibolites of the Série Negra in the vicinity of São Martinho are mostly hidden below a Palaeogenic clast-supported elluvium deposit that covers most of the area. Hence, in this area studies have mostly to resort to borehole samples. However, on the edges of this deposit further to the SSW of trig. beacon São Martinho (figure 1; location of sample DP91), small (< 2m-wide) outcrops of amphibolite occur. The best exposure of amphibolites and banded amphibolites is in the railway cutting

ESE of trig. beacon Travesso (figure 1; locations of samples DP42 and 43). Here the amphibolitic rock outcrops are dominantly massive (with local banding) in character with a dark colour and locally with ferruginous staining when slightly weathered. They outcrop adjacent to quartz-biotite schists, and black quartzites of the Série Negra and are intruded by aplitic veins, rhyolites and several apophyses of the Barreiros tectonised granitoid (figure 2.10 *in* de OLIVEIRA, 2001). Further to the E, near Assumar, the distinct banding of the banded amphibolites is more evident although outcrops are limited to small occurrences in road cuttings or stream beds.

Two phases of Variscan deformation are identified in this sector (GONÇALVES *et al.*, 1972a, b). The first phase of deformation (D1) develops folds with WSW verging axial planar schistosity (S1) with a tendency of the axial planes becoming more horizontal as one moves southwards. The second phase of deformation (D2) generated folds with subvertical axial planes or strongly dipping to the NE and striking NW-SE. D2 deformation generates refolding of the D1 structures and develops crenulation cleavage (S2) [PEREIRA, 1995].

The TCSZ is intruded by several pre-Hercynian [e.g. the Late Cambrian (weighted mean $^{207}\text{Pb}/^{206}\text{Pb}$ age of 508 ± 8.1 Ma) Barreiros tectonised granitoids, de OLIVEIRA *et al.*, 2002; the (ultra)basic to felsic intrusions of Alter do Chão-Cabeço de Vide, Campo Maior and Elvas), syn-Hercynian (e.g. the as yet to be dated elongated granitoid bodies E of Alter do Chão; figure 1) and late- to post-

Hercynian rocks (e.g. the Nisa and Santa Eulália granite batholiths).

3. PREAMBLE

In order to follow our approach, a brief review of field and microscopic features of the amphibolitic rocks follows. Amphibolites are rather massive metamorphic rocks composed chiefly of hornblende and plagioclase (with $An \geq 17$) and are diagnostic of the amphibolite facies of metamorphism. They are amongst the most common rocks formed by regional metamorphism of moderate-to-high-grade (WILLIAMS *et al.*, 1982). Amphibolite facies metamorphism applies over a temperature range of approximately 500-650 °C and pressures of 3-10 kb (figure 2.1 *in* SHELLEY, 1995).

Amphibolite protoliths are commonly basalt, dolerite and gabbro. Banded amphibolites can be formed from a variety of rocks mostly from (ultra)basic to intermediate igneous rocks but also from impure calcareous and dolomitic sedimentary rocks (HYNDMAN, 1985).

In thin section amphibolites show a preferred orientation of the hornblende prisms (WILLIAMS *et al.*, 1982) defining a schistosity, a lineation or both (SPRY, 1969; SHELLEY, 1995), better defined in the banded amphibolites, where it is also well expressed mesoscopically. Banding in the banded amphibolites may be produced by segregation of constituents during recrystallisation or, alternatively, may be inherited from bedding or layering in sedimentary or igneous rocks, respectively (BATES & JACKSON, 1987).

4. DEFINITION WITHIN THE STUDY AREA

Within the study area the distinction is made between amphibolite and banded amphibolite. This distinction stems from the more pervasive and penetrative schistosity (parallel to the schistosity in enclosing quartz-biotite schists) of the banded amphibolites *vs.* the more massive, homogeneous character of the amphibolites at the outcrop scale. The banded amphibolites show better-defined segregation of quartz and plagioclase crystals into discrete bands. Figure 3 exemplifies these features. However, these two lithologies often grade into each other and no sharp contacts between banded amphibolites and amphibolites are seen. Banded amphibolites extend for up to tens of metres within either amphibolites or quartz biotite schists. Though both banded amphibolites and amphibolites host gold mineralisation, it is more common in the former.

5. MINERALOGY AND TEXTURES

The mineralogy of the amphibolites is generally similar in samples collected from outcrops and from trenches and boreholes. The only real difference between samples is the amount of alteration these have suffered as a result of the various prograde and retrograde metamorphic events.

In both the amphibolites and banded amphibolites the grain size is extremely heterogeneous and can range from 10 µm to 250 µm in diameter. This value takes into account not only the amphibole size but also that of quartz, plagioclase and epidote (when present).

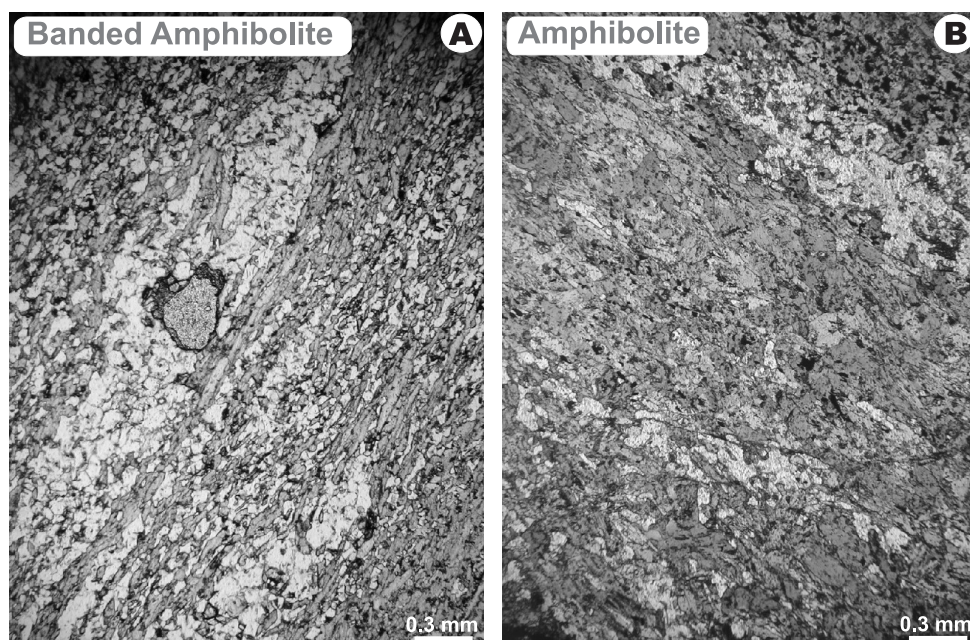


Figure 3. Photomicrographs highlighting the textural differences between banded amphibolite (A) and amphibolite (B). The former has a strongly developed schistosity with clear separation between alternating quartz/feldspar-rich bands (light) and amphibole-rich bands (dark) while the latter has a distinctly massive character. (Adapted after de OLIVEIRA, 2001).

Mineralogically the banded amphibolites are made up of amphibole, plagioclase plus minor quartz with titanite and apatite with very few opaques set in a nematoblastic texture. No biotite was observed in the thin sections but discrete bands of biotite from intervening schists have been observed in borehole core. Microchemical analyses of the hornblendes and feldspars (average analyses shown in appendix 1 and appendix 2 respectively) allow these minerals to be classified, respectively, as predominantly magnesiohornblende (with a weak shift towards the actinolite and tschermakite fields) (figure 4A) and predominantly labradorite with a reduced num-

ber of samples also falling in the andesine and bytownite fields (figure 4B).

The amphibolites are more massive and consist of strongly coloured amphibole with mostly untwinned xenoblastic plagioclase, epidote plus minor quartz, titanite, magnetite, ilmenite and rare rutile. Garnet is common in higher-grade amphibolites (SHELLEY, 1995), but these have only been found in one sample near Assumar in a hornblende-garnet schist (sample DP69, figure 1; de OLIVEIRA, 2001,) gneiss similar to an amphibolite in mineralogy but interpreted as a retrogressed eclogite by PEREIRA (1999). Microprobe analyses of the amphiboles

and feldspars in the studied amphibolites allow these minerals to be classified as actinolite-magnesiohornblende, while the feldspars range from oligoclase to bytownite clustering into a oligoclase-andesine group and a different labradorite-bytownite group (figures 4A and B), both amphibole and plagioclase diagrams being distinct from the banded amphibolites case.

From this purely mineralogical point of view it would seem that both amphibolites and banded amphibolites in this area could be derived from basic protoliths. However, other alternative protoliths for the latter would also have to be suggested, since the presence in the banded amphibolites of discrete biotite bands may indicate a possible tuffaceous protolith (WILLIAMS *et al.*, 1982) and in other cases, thin, variable bands rich in quartz, (carbonates) and biotite suggest a sedimentary origin (SHELLEY, 1995).

6. GEOCHEMISTRY

6.1. Methodology

The samples were analysed by X-ray Fluorescence (XRF) at the Dept. of Geology, University of the Witwatersrand in Johannesburg using a Philips PW 1400 with a rhodium X-ray tube at 50kV and 50mA. Strict quality control for major elements was done using the method laid out by NORRISH & HUTTON (1969) while quality control for the trace elements was carried out using the method laid out by FEATHER & WILLIS (1976). Absolute percentage errors and the standard deviation are set out in table 1.

6.2. Protolith signatures through geochemistry

Since the contacts between the amphibolites and banded amphibolites are gradational, the geochemical analyses refer mostly to amphibolites and only in three cases where clear meso- and microscopic textural relationships were observed, banded amphibolites were analysed. All samples were free of analysis-contaminating features, e.g. quartz veins.

Geochemically these rocks range from intermediate to basic in terms of their SiO₂ content (table 1). Several plots, shown in figure 5, highlight some of the relationships obtained for these rocks in terms of their possible protoliths and tectonic setting.

Using volcanic rock nomenclature diagrams, all samples plot in the basic fields of the diagrams shown by figures 5A and B. The diagram in figure 5A shows a spread of the amphibolite samples from the alkaline basalt to subalkaline basalt fields while the samples of the banded amphibolites plot on the border between the andesite/basalt and subalkaline basalt fields. The diagram in figure 5B mirrors the spread of amphibolite samples across the basalt and basalt-andesite fields whereas the banded amphibolites all plot within the basalt field. This approach corroborates, in a way, the previous considerations about a dominant basic protolith for these rocks.

In order to evaluate the possible magma type the amphibolites may have been derived from, the set of samples has been plotted on the FeO(t)-(Na₂O+K₂O)-MgO (AFM) diagram (figure 5C). The spread of

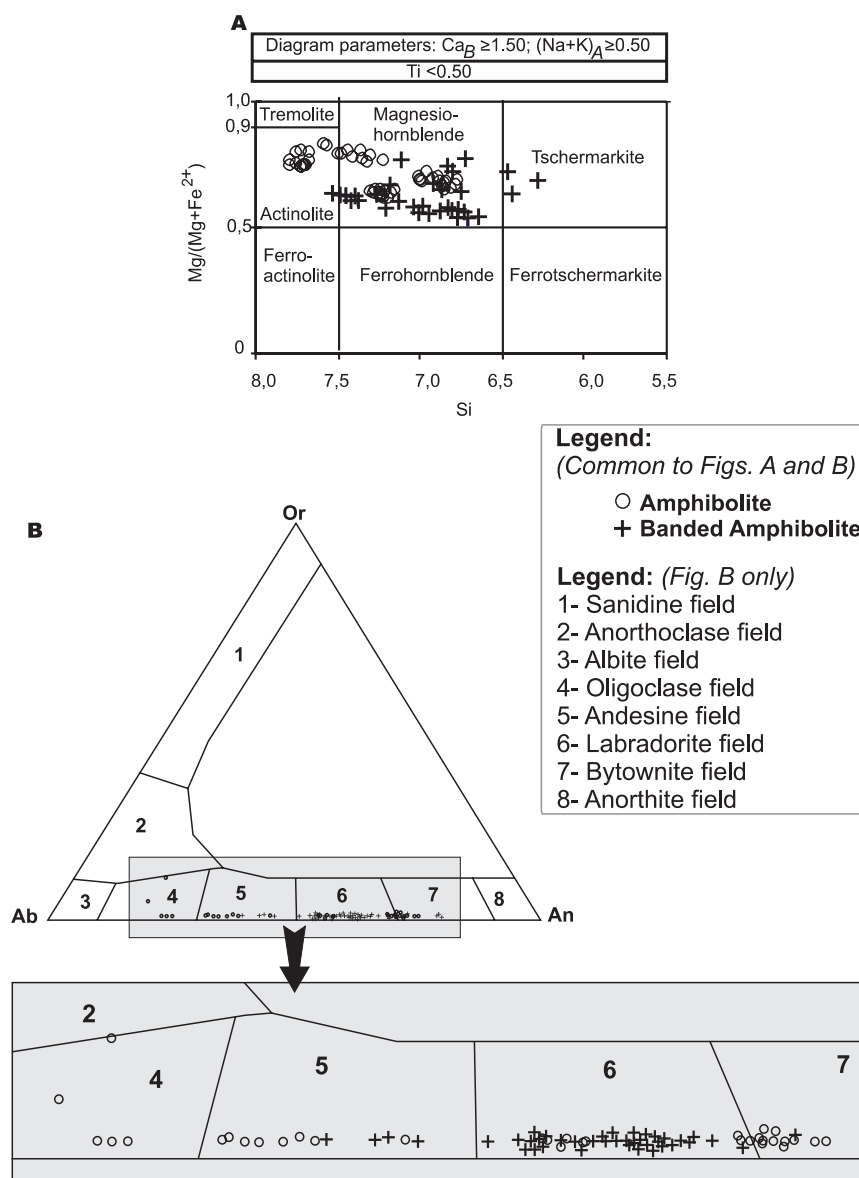


Figure 4. A- Mineral classification diagram for the calcic amphiboles in amphibolite *vs.* banded amphibolite. Although both sets of amphiboles plot on the same field of the LEAKE *et al.* (1997) diagram, the amphiboles in the banded amphibolite, mostly classified as magnesiohornblende, while the amphiboles in the amphibolites cluster loosely across the actinolite and magnesiohornblende fields. B- Classification diagram for the feldspars in the amphibolites and banded amphibolites. The distribution of the types of feldspars that occur in the two lithologies is different. All diagrams plotted from data whose averages are shown in appendices 1 and 2.

the amphibolite samples across both the tholeiitic and calc-alkaline fields of the diagram is observed. The banded amphibolite samples group tightly within the tholeiitic field (figure 5C). The diagram in figure 5D shows a plot of the samples with respect to their possible tectonic setting, tentatively

suggesting a within-plate versus a more MORB tectonic setting for amphibolites and banded amphibolites, respectively. However, the large scatter and lack of discrete grouping in any of the designated fields makes this diagram hard to interpret and is not conclusive.

Amphibolite								
	DP5	DP68	DP69	DP91	T16/2/50	T16/2/53	T16/2/77	T0/245
SiO ₂	50.13	50.16	46.61	51.11	57.03	55.44	55.30	56.10
TiO ₂	3.13	2.18	2.70	1.23	0.50	1.39	1.88	1.15
Al ₂ O ₃	13.46	14.68	14.18	15.89	7.50	8.04	15.69	16.14
Fe ₂ O ₃	15.54	12.17	13.55	9.70	7.09	8.54	6.57	8.84
MnO	0.30	0.26	0.20	0.16	0.32	0.25	0.12	0.11
MgO	4.67	7.79	6.63	6.95	10.55	11.13	4.56	5.12
CaO	8.31	8.18	10.45	10.44	14.37	10.81	9.21	6.78
Na ₂ O	3.16	2.83	2.60	2.88	1.35	0.37	3.25	3.17
K ₂ O	0.53	0.39	0.90	0.35	0.73	1.38	0.55	0.57
P ₂ O ₅	0.42	0.23	0.36	0.09	0.19	0.48	0.65	0.11
LOI	0.62	1.56	0.78	1.33	0.78	2.63	2.68	2.20
<i>total</i>	<i>100.26</i>	<i>100.43</i>	<i>98.95</i>	<i>100.14</i>	<i>100.42</i>	<i>100.48</i>	<i>100.45</i>	<i>100.63</i>
Y	58	40	37	26	6	35	34	23
Zr	236	137	211	60	78	308	361	109
Nb	12	8	22	6	14	50	50	8

Banded amphibolite				<i>Element</i>	<i>Std. Dev.</i>	<i>Absolute % error</i>
	DP43	DP85	DP87	<i>SiO₂</i>	<i>0.07</i>	<i>-0.031</i>
SiO ₂	50.84	46.62	50.53	<i>TiO₂</i>	<i>0.01</i>	<i>-0.006</i>
TiO ₂	0.99	1.84	1.55	<i>Al₂O₃</i>	<i>0.07</i>	<i>-0.041</i>
Al ₂ O ₃	16.48	12.75	13.90	<i>Fe₂O₃</i>	<i>0.06</i>	<i>0.004</i>
Fe ₂ O ₃	9.96	15.63	11.31	<i>MnO</i>	<i>0.07</i>	<i>-0.002</i>
MnO	0.15	0.23	0.14	<i>MgO</i>	<i>0.02</i>	<i>-0.017</i>
MgO	6.52	6.86	7.41	<i>CaO</i>	<i>0.41</i>	<i>-0.043</i>
CaO	11.12	10.41	11.57	<i>Na₂O</i>	<i>0.41</i>	<i>-0.218</i>
Na ₂ O	2.33	2.87	2.46	<i>K₂O</i>	<i>0.17</i>	<i>-0.050</i>
K ₂ O	0.29	0.32	0.19	<i>P₂O₅</i>	<i>0.10</i>	<i>0.060</i>
P ₂ O ₅	0.07	0.16	0.15	<i>LOI</i>	<i>0.26</i>	<i>-0.153</i>
LOI	1.12	0.85	0.87	<i>total</i>	<i>0.500</i>	<i>-0.340</i>
<i>total</i>	<i>99.86</i>	<i>98.55</i>	<i>100.08</i>	<i>SiO₂</i>	<i>0.07</i>	<i>-0.031</i>
Y	24	43	36	<i>Element</i>	<i>Std. Dev.</i>	<i>Absolute error -ppm</i>
Zr	67	111	97	<i>Y</i>	<i>2</i>	<i>-0.2</i>
Nb	7	8	7	<i>Zr</i>	<i>5</i>	<i>1.9</i>
				<i>Nb</i>	<i>1</i>	<i>-2.2</i>

Table 1. Major and selected minor element geochemistry used for generating figures 5A, B, C and D. Fe₂O₃ was converted to FeO(t) and all major element values recalculated to 100% for the purposes of plotting the AFM diagram. Major element values expressed in wt% and minor element values in ppm. Absolute errors for analytical methods are shown: average of 5 calibrations for major elements and 3 calibrations for trace elements.

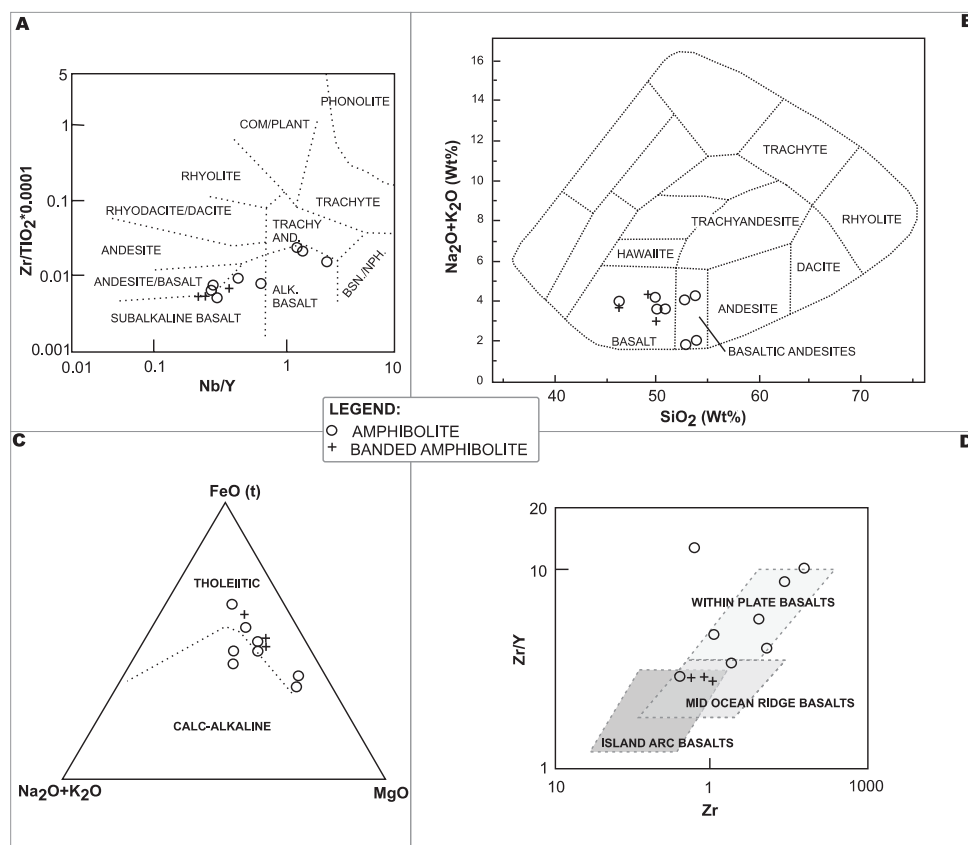


Figure 5. Geochemical relationships (after de OLIVEIRA, 2001) obtained for banded amphibolites and amphibolites. Figures A and B deal with the nomenclature of the various rocks (A - after WINCHESTER & FLOYD, 1977; B - after COX *et al.*, 1979). The discrimination of tholeiitic from calc-alkaline series is shown in the AFM diagram (C - after KUNO, 1968). The Zr/Zr-Y diagram for discriminating between within-plate, MORB and arc basalts is shown in D (after PEARCE AND NORRY, 1979).

7. DISCUSSION

Amphibolite and banded amphibolite constitute a suite of rocks that are clearly distinguishable in the field on a mesoscopic scale. However, the above mentioned approaches and results, as well as the analytical data show that these rocks have a high degree of variability that is dependant on the mineralogy of each individual sample.

Geochemical data are inconclusive with respect to establishing a tectonic setting perhaps due to an insufficient number of samples collected. The observed geochemistry and mineralogy indicate a probable basic protolith for both amphibolites and banded amphibolites, but the protolith could be more variable for the latter since they may also exist textures akin those found in rocks of sedimentary-

tuffaceous origin as exemplified by the presence, in the banded amphibolites, of both discrete biotite layers and also the abundance of distinct amphibole-rich layers juxtaposed by plagioclase and quartz layers. Therefore, perhaps, this suite of rocks should be generically treated as amphibolite (*s.l.*) from a geochemical point of view but from a textural and mineralogical point of view these amphibolite and banded amphibolite should be treated as individual entities as they have been and continue to be by exploration geologists working in the area and in all the Ossa Morena Zone.

ACKNOWLEDGEMENTS

This work represents a small part of a much larger Ph.D. undertaken at the University of the Witwatersrand (Republic of South Africa) by the senior

author and supervised by the second and fourth authors. We would like to acknowledge the contribution of Prof. F. M. Meyer of the *Institut für Mineralogie und Lagerstättenlehre* (Aachen, Germany) in supplying microprobe facilities and R. Solá of the IGM who helped with the diagrams. The senior author benefited from a *Praxis XXI PhD bursary (BD/15877/98)* awarded by the *Fundação para a Ciência e a Tecnologia*. Messrs. A. Gouveia and A. Verde are thanked for polished thin section preparation. Mr. J. L. Pinto is thanked for help with sample collection and field work.

Recibido: 07-XI-02

Aceptado: 20-I-03

	Amphiboles in amphibolite				Amphiboles in banded amphibolite			
	DP68 Avg. n= 14	DP91 Avg. n= 15	T16/2/50 Avg. n= 10	T6/2/3 Avg. n= 13	DP42 Avg. n= 10	DP43 Avg. n= 12	DP85 Avg. n= 8	DP87 Avg. n= 8
Average	44.513	46.370	50.143	46.440	44.513	46.370	50.143	46.440
SiO ₂	0.529	0.447	0.292	0.475	0.529	0.447	0.292	0.475
TiO ₂	9.431	9.807	5.327	8.754	9.431	9.807	5.327	8.754
Al ₂ O ₃	18.223	14.209	14.658	15.875	18.223	14.209	14.658	15.875
Cr ₂ O ₃	0	0	0	0	0	0	0	0
MnO	0.364	0.303	0.256	0.281	0.364	0.303	0.256	0.281
MgO	9.837	12.638	12.741	10.808	9.837	12.638	12.741	10.808
CaO	11.885	11.603	12.175	12.183	11.885	11.603	12.175	12.183
Na ₂ O	1.132	1.207	0.558	0.907	1.132	1.207	0.558	0.907
K ₂ O	0.249	0.037	0.124	0.247	0.249	0.037	0.124	0.247
F	0.025	0.047	0.029	0.056	0.025	0.047	0.029	0.056
Cl	0	0	0	0	0	0	0	0
Total	96.190	96.670	96.300	96.030	96.190	96.670	96.300	96.030
<i>Structural formula</i>								
O F Cl	0.01	0.02	0.01	0.02	0.01	0.02	0.01	0.02
Ctotal								
TSi	6.729	6.798	7.117	6.971	6.729	6.798	7.117	6.971
TAl	1.271	1.202	0.583	1.029	1.271	1.202	0.583	1.029
TFe3	0	0	0	0	0	0	0	0
TTi	0	0	0	0	0	0	0	0
Sum T	8	8	8	8	8	8	8	8
CAI	0.408	0.492	0.345	0.518	0.408	0.492	0.345	0.518
CCr	0	0	0	0	0	0	0	0
CFe3	0.444	0.450	0.090	0.136	0.444	0.450	0.090	0.136
CTi	0.060	0.049	0.032	0.054	0.060	0.049	0.032	0.054
CMg	2.217	2.762	2.810	2.419	2.217	2.762	2.810	2.419
CFe2	1.849	1.228	1.707	1.856	1.849	1.228	1.707	1.856
CMn	0.023	0.019	0.016	0.018	0.023	0.019	0.016	0.018
CCa	0	0	0	0	0	0	0	0
Sum C	5	5	5	5	5	5	5	5
BMg	0	0	0	0	0	0	0	0
BFe2	0.012	0.064	0.017	0.001	0.012	0.064	0.017	0.001
BMn	0.023	0.019	0.016	0.018	0.023	0.019	0.016	0.018
BCa	1.925	1.823	1.93	1.959	1.925	1.823	1.93	1.959
BNa	0.040	0.094	0.038	0.022	0.040	0.094	0.038	0.022
Sum_B	2	2	2	2	2	2	2	2
ANa	0	0	0	0	0	0	0	0
ANa	0.292	0.249	0.122	0.242	0.292	0.249	0.122	0.242
AK	0.048	0.007	0.023	0.047	0.048	0.007	0.023	0.047
Sum A	0.340	0.256	0.146	0.289	0.340	0.256	0.146	0.289
Sum_cat	15.340	15.256	15.146	15.289	15.340	15.256	15.146	15.289
CCl	0	0	0	0	0	0	0	0
CF	0.012	0.022	0.013	0.027	0.012	0.022	0.013	0.027
Sum oxy	23	23	23	23	23	23	23	23

Appendix 1. Average microanalytical data for amphiboles. Structural formula calculated on an anhydrous basis to cations per 23O after RICHARD & CLARKE (1990); Fe²⁺ and Fe³⁺ calculated after ROBINSON *et al.* (1981). [Probe: JEOL JXA.8900R; 25 nA beam current; 15 kV accelerating voltage; 1 µm beam diameter; 10 and 5s counting times (peak and background respectively)].

Feldspars in amphibolite					Feldspars in banded amphibolite				
	DP68	DP91	T16/2/50-A	T16/2/50-B		DP42	DP43	DP85	DP87
	Avg.n-13	Avg.n-11	Avg.n-3	Avg.n-7		Avg.n-14	Avg.n-10	Avg.n-10	Avg.n-10
SiO ₂	62.01	60.89	61.29	57.41	SiO ₂	58.91	57.00	59.83	58.45
Al ₂ O ₃	23.34	24.44	24.02	26.54	Al ₂ O ₃	26.17	26.87	25.39	26.02
TiO ₂	0.00	0.00	0.00	0.00	TiO ₂	0.00	0.00	0.00	0.00
FeO	0.09	0.27	0.06	0.03	FeO	0.10	0.03	0.26	0.14
MnO	0.00	0.00	0.00	0.00	MnO	0.00	0.00	0.00	0.00
MgO	0.00	0.00	0.00	0.00	MgO	0.00	0.00	0.00	0.00
CaO	5.54	5.46	5.29	7.77	CaO	7.31	8.84	6.69	7.62
Cr ₂ O ₃	0.00	0.00	0.00	0.00	Cr ₂ O ₃	0.00	0.00	0.00	0.00
P ₂ O ₅	0.00	0.00	0.00	0.00	P ₂ O ₅	0.00	0.00	0.00	0.00
Na ₂ O	6.48	7.95	7.83	6.17	Na ₂ O	7.00	6.32	7.41	6.57
K ₂ O	0.21	0.07	0.17	0.70	K ₂ O	0.06	0.06	0.05	0.21
Total	97.68	99.33	98.95	99.03	Total	99.74	99.32	99.81	99.21
<i>Structural formula (8 O)</i>					<i>Structural formula (8 O)</i>				
Si	2.79	2.72	2.75	2.60	Si	2.64	2.57	2.67	2.63
Al	1.24	1.29	1.27	1.42	Al	1.38	1.43	1.34	1.38
Fe	0.00	0.01	0.00	0.00	Fe	0.00	0.00	0.01	0.01
Ca	0.27	0.26	0.25	0.38	Ca	0.35	0.43	0.32	0.37
Na	0.57	0.69	0.68	0.54	Na	0.61	0.55	0.64	0.57
K	0.01	0.00	0.01	0.04	K	0.00	0.00	0.00	0.01
P	0.00	0.00	0.00	0.00	P	0.00	0.00	0.00	0.00
Cr	0.00	0.00	0.00	0.00	Cr	0.00	0.00	0.00	0.00
Mg	0.00	0.00	0.00	0.00	Mg	0.00	0.00	0.00	0.00
Mn	0.00	0.00	0.00	0.00	Mn	0.00	0.00	0.00	0.00
Sum	4.88	4.98	4.96	4.98	Sum	4.98	4.99	4.98	4.97
<i>Mol %</i>					<i>Mol %</i>				
%An	31.62	27.40	26.90	39.29	%An	36.48	43.45	33.18	38.59
%Ab	66.93	72.20	72.08	56.47	%Ab	63.19	56.21	66.52	60.18
%Or	1.45	0.40	1.02	4.23	%Or	0.33	0.34	0.30	1.24

Appendix 2. Average microanalytical data for feldspar. (Probe data as per appendix 1).

REFERENCES

- ABALOS, B. & EGUILUZ, L. (1992). Evolución geodinámica de la zona de cisalla dúctil de Badajoz-Córdoba durante el Proterozoico Superior-Cámbrico Inferior. In: *Paleozoico inferior de Ibero-América*, Gutiérrez-Marco, J.C.; Saavedra, J. & Rábano, I. (eds.), Universidad de Extremadura, pp.: 577-591.
- BATES, R. L. & JACKSON, J. A. (eds.) (1987). *Glossary of Geology*, 3rd Ed., American Geological Institute, Alexandria, Virginia, Thompson Shore, Inc., 788 pp.
- BERTHÉ, D.; CHOUKROUNE, P. & JEGOUZO, P. (1979). Orthogneiss, mylonite and non coaxial deformation granites: the example of the south Armorican shear zone. *Journal of Structural Geology*, 1: 31-42.
- BURG, J. P.; IGLESIAS, M.; LAURENT, P. H.; MATTE, P. & RIBEIRO, A. (1981). Variscan intracontinental deformation: The Coimbra-Córdoba Shear Zone (SW Iberian Peninsula). *Tectonophysics*, 78: 161-177.
- COX, K. G.; BELL, J. D. & PANKHURST, R. J. (1979). *The interpretation of igneous rocks*. George, Allen and Unwin, London, 450 pp.
- de OLIVEIRA, D. P. S. (1998). The rare earth-bearing Llandeilian quartzites in the Vale de Cavalos-Portalegre area, Central Iberian Zone, Portugal - Their better understanding through geological mapping and rock geochemistry. *Comunicações, Actas do V Congresso Nacional de Geologia*, 84 (1): B142-B145.
- de OLIVEIRA, D. P. S. (2001). *The nature and origin of gold mineralisation in the Tomar Cordoba Shear Zone, Ossa Morena Zone, Eastern Portugal*. Ph.D. Thesis (Unpubl.), University of the Witwatersrand, Republic of South Africa, 352 pp.
- de OLIVEIRA, D. P. S.; POUJOL, M. & ROBB, L. J. (2002). U-Pb geochronology for the Barreiros tectonised granitoids and Arronches migmatitic gneisses: Tomar Cordoba Shear Zone, east central Portugal. *Rev. Soc. Geol. España*, 15 (1-2): 105-112.
- FEATHER, C. E. & WILLIS, J. P. (1976). A simple method for background and matrix correction of spectral peaks in trace element determination by X-Ray fluorescence spectrometry. *X-Ray Spectrometry*, 5: 44-48.
- GONÇALVES, F.; ASSUNÇÃO, C. T. & COELHO, A. V. P. (1972a). *Notícia explicativa da folha 33-C (Campo Maior)*. Serviços Geológicos de Portugal.
- GONÇALVES, F.; PELEJA, A. F. & JARDIM, J. J. (1972b). *Geological map of Portugal, Sheet 32-B (Portalegre), Scale 1:50000*. Serviços Geológicos de Portugal.
- HYNDMAN, D. W. (1985). *Petrology of igneous and metamorphic rocks*, 2nd. Ed. Mcgraw-hill Book Company, 786 pp.
- KUNO, H.; (1968). Differentiation of basalt magmas. In: Hess, H.H. and Poldervaart, A. (eds.), *Basalts: The Poldervaart Treatise on Rocks of Basaltic Composition*, Vol. 2. Interscience, New York, pp.: 623-688.
- LEAKE, B. E.; WOOLEY, A. R.; ARPS, C. E. S.; BIRCH, W. D.; GILBERT, M. C.; GRICE, J. D.; HAWTHORNE, F. C.; KATO, A.; KISCH, H. J.; KRIVOVICHEV, V. G.; LINHOUT, K.; LAIRD, J.; MANDARINO, J. A.; MARESH, W. V.; NICKEL, E. H.; ROCK, N. M. S.; SCHUMACHER, J. C.; SMITH, D. C.; STEPHENSON, N. C. N.; UNGARETTI, L.; WITAKER, E. J. W. & YOUZHI, G. (1997). Nomenclature of amphiboles: Report of the subcommittee on amphiboles of the international mineralogical association, commission on new minerals and mineral names. *The Canadian Mineralogist*, 35: 219-246.
- NORRISH, K. & HUTTON, J. T. (1969). An accurate X-ray spectrographic method for the analysis of a wide range of geological samples. *Geochimica et Cosmochimica Acta*, 33 (4): 431-453.
- OLIVEIRA, J. T.; OLIVEIRA, V. & PIÇARRA, J. M. (1991). Traços gerais da evolução tectonoestratigráfica da Zona de Ossa Morena. *Comunicações Serviços Geológicos Portugal*, 77: 3-26.
- OLIVEIRA, J. T.; PEREIRA, E.; RAMALHO, M.; ANTUNES, M. T. & MONTEIRO, J. H. (1992). *Carta Geológica de Portugal 1:500000*. Serviços Geológicos de Portugal.
- ORDOÑES-CASADO, B. (1998). *Geochronological studies of the Pre-Mesozoic basement of the Iberian Massif: The Ossa Morena Zone and the allocthonous complexes within the Central Iberian Zone*. PhD thesis, Swiss Federal Institute of Technology Zürich, ETH N° 12.940, 233 pp.
- PEARCE, J. A. & NORRY, M. J. (1979). Petrogenic implications of Ti, Zr, Y and Nb

- variations in volcanic rocks. *Contributions to Mineralogy and Petrology*, 69: 33-47.
- PEREIRA, M. F. C. de C. (1995). *Estudo tectónico da megaestrutura de Crato-Arronches-Campo Maior: A Faixa Blastomilonítica e limite setentrional da Zona de Ossa Morena com o autóctone Centro Ibérico (Nordeste Alentejano)*. MSc thesis (unpubl.), Faculty of Science; University of Lisbon, 108 pp.
- PEREIRA, M. F. C. de C. (1999). *Caracterização da estrutura dos domínios setentrionais da Zona de Ossa Morena e seu limite com a Zona Centro Ibérica, no nordeste alentejano*. Ph.D. thesis (unpubl.), University of Évora, 114 pp.
- PEREIRA, M. F. & SILVA, J. B. (2001). A new model for the Hercynian Orogen of Gondwanan France and Iberia: discussion. *Journal of Structural Geology*, 23: 835-838.
- QUESADA, C. & MUNHÁ, J. (1990). Metamorphism. In: *Pre-Mesozoic Geology of Iberia*, Dallmeyer, R.D. & Martinez Garcia, E. (eds.), Springer Verlag Berlin Heidelberg, pp.: 314-319.
- RICHARD, L. R. & CLARKE, D. B. (1990). AMPHIBOL: A program for calculating structural formulae and for classifying and plotting analyses of amphiboles. *American Mineralogist*, 75: 421-423.
- ROBINSON, P.; SPEAR, F. S.; SCHUMACHER, J. C.; LAIRD, J.; KLEIN, C.; EVANS, B. W. & DOOLAN, B. L. (1981). Phase relations of metamorphic amphiboles: Natural occurrence and theory. *Mineralogical Society of America-Reviews in Mineralogy*, 9B: 1-228.
- SCHÄFER, H. J.; GEBAUER, D.; NAGLER, T. F. & EGUILUZ, L. (1993). Conventional and ion-microprobe U-Pb dating of detrital zircons of the Tentudía Group (Série Engra, SW Spain): implications for zircon systematics, stratigraphy, tectonics and the Precambrian/Cambrian boundary. *Contributions to Mineralogy and Petrology*, 113: 289-299.
- SHELLEY, D. (1995). *Igneous and metamorphic rocks under the microscope. Classification, textures, microstructures and mineral preferred orientations*. Chapman & Hall, 445 pp.
- SPRY, A. (1969). *Metamorphic Textures*. Pergamon Press, 360 pp.
- WILLIAMS, H.; TURNER, F. J. & GILBERT, C. M. (1982). *Petrography. An introduction to the study of rocks in thin sections* (2nd Ed.). W.H. Freeman and Company, S. Francisco, 626 pp.
- WINCHESTER, J. A. & FLOYD, P. A. (1977). Geochemical discrimination of different magma series and their differentiation products using immobile elements. *Chemical Geology*, 20: 325-343.